Chapter 2
Mechanics of the Wheel with Tire

All road vehicles have wheels and almost all of them have *wheels* with *pneumatic tires*. Wheels have been around for many centuries, but only with the invention, and enhancement, of the pneumatic tire it has been possible to conceive fast and comfortable road vehicles [3].

The main features of any tire are its *flexibility* and *low mass*, which allow for the contact with the road to be maintained even on uneven surfaces. Moreover, the rubber ensures *high grip*. These features arise from the highly composite structure of tires: a carcass of flexible, yet almost inextensible cords encased in a matrix of soft rubber, all inflated with air.[1] Provided the (flexible) tire is properly inflated, it can exchange along the bead relevant actions with the (rigid) rim. Traction, braking, steering and load support are the net result.

It should be appreciated that the effect of air pressure is to increase the structural stiffness of the tire, not to support directly the rim. How a tire carries a vertical load F_z if properly inflated is better explained in Fig. 2.1. In the lower part, the sidewalls bend and, thanks to the air pressure p_a, they apply more vertical forces F_a in the bead area than in the upper part. The overall effect on the rim is a vertical load F_z. The higher the air pressure p_a, the lower the sidewall bending.

The *contact patch*, or footprint, of the tire is the area of the tread in contact with the road. This is the area that transmits forces between the tire and the road via pressure and friction. To truly understand some of the peculiarities of tire mechanics it is necessary to get some insights on what happens in the contact patch.

Handling of road vehicles is strongly affected by the mechanical behavior of the wheels with tire, that is by the *relationship* between the *kinematics* of the rigid rim and the *force* exerted by the road. This chapter is indeed devoted to the analysis of experimental tests. The development of simple, yet significant, tire models is done in Chap. 10.

[1] Only in competitions it is worthwhile to employ special (and secret) gas mixtures instead of air. The use of nitrogen, as often recommended, is in fact completely equivalent to air, except for the cost.

M. Guiggiani, *The Science of Vehicle Dynamics*, DOI 10.1007/978-94-017-8533-4_2,

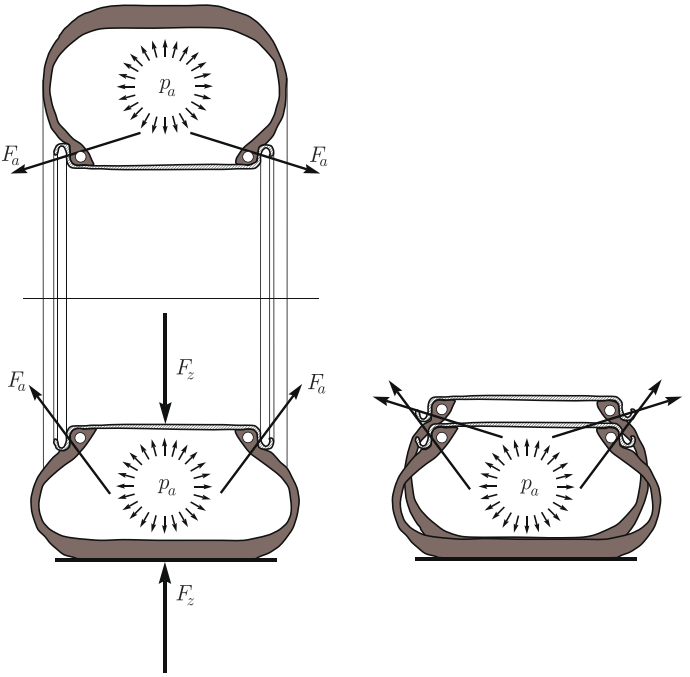

Fig. 2.1 How a tire carries a vertical load if properly inflated

2.1 The Tire as a Vehicle Component

A wheel with tire is barely a wheel, in the sense that it behaves quite differently from a rigid wheel.[2] This is a key point to really understand the mechanics of wheels with tires. For instance, a rigid wheel touches the (flat) road at one point C, whereas a tire has a fairly large contact patch. Pure rolling of a rigid wheel is a clear kinematic concept [12], but, without further discussion, it is not obvious whether an analogous concept is even meaningful for a tire. Therefore, we have to be careful in stating as clearly as possible the concepts needed to study the mechanics of wheels with tire.

Moreover, the analysis of tire mechanics will be developed with no direct reference to the dynamics of the vehicle. This may sound a bit odd, but it is not. The goal here is to describe the *relationship* between the *motion* and *position* of the rim and the *force* exchanged with the road through the contact patch:

$$\text{rim kinematics} \quad \Longleftrightarrow \quad \text{force and moment}$$

[2] A rigid wheel is essentially an axisymmetric convex rigid surface. The typical rigid wheel is a toroid.

Once this description has been obtained and understood, then it can be employed as one of the fundamental components in the development of suitable models for vehicle dynamics, but this is the subject of other chapters.

Three basic components play an active role in tire mechanics:

(1) the *rim*, which is assumed to be a rigid body;
(2) the flexible *carcass* of the inflated tire;
(3) the *contact patch* between the tire and the road.

2.2 Rim Position and Motion

For simplicity, the *road* is assumed to have a hard and *flat* surface, like a *geometric plane*. This is a good model for any road with high quality asphalt paving, since the texture of the road surface is not relevant for the definition of the rim kinematics (while it highly affects grip [8]).

The *rim* $\mathscr{R}$ is assumed to be a *rigid body*, and hence, in principle, it has six degrees of freedom. However, only two degrees of freedom (instead of six) are really relevant for the rim *position* because the road is *flat* and the wheel rim is *axisymmetrical*.

Let Q be a point on the rim axis y_c (Fig. 2.2). Typically, although not strictly necessary, a sort of midpoint is taken. The *position* of the rim with respect to the flat road depends only on the *height* h of Q and on the *camber angle* γ (i.e., the inclination) of the rim axis y_c. More precisely, h is the distance of Q from the road plane and γ is the angle between the rim axis and the road plane.

Now, we can address how to describe the rim velocity field.

The rim, being a rigid body, has a well defined angular velocity $\mathbf{\Omega}$. Therefore, the velocity of any point P of the (space moving with the) rim is given by the well known equation [7, p. 124]

$$\mathbf{V}_P = \mathbf{V}_Q + \mathbf{\Omega} \times QP \tag{2.1}$$

where $\mathbf{V}_Q$ is the velocity of Q and QP is the vector connecting Q to P. The three components of $\mathbf{V}_Q$ and the three components of $\mathbf{\Omega}$ are, e.g., the *six* parameters which completely determine the rim *velocity* field.

A moving reference system $\mathsf{S} = (x, y, z; O)$ is depicted in Fig. 2.2. It is defined in a fairly intuitive way. The y-axis is the intersection between a vertical plane containing the rim axis y_c and the road plane. The x-axis is given by the intersection of the road plane with a plane containing Q and normal to y_c. Axes x and y define the origin O as a point on the road. The z-axis is vertical, that is perpendicular to the road, with the positive direction upward.[3] The unit vectors marking the positive directions are $(\mathbf{i}, \mathbf{j}, \mathbf{k})$, as shown in Fig. 2.2.

[3] S is the system recommended by ISO (see, e.g., [14, Appendix 1]).

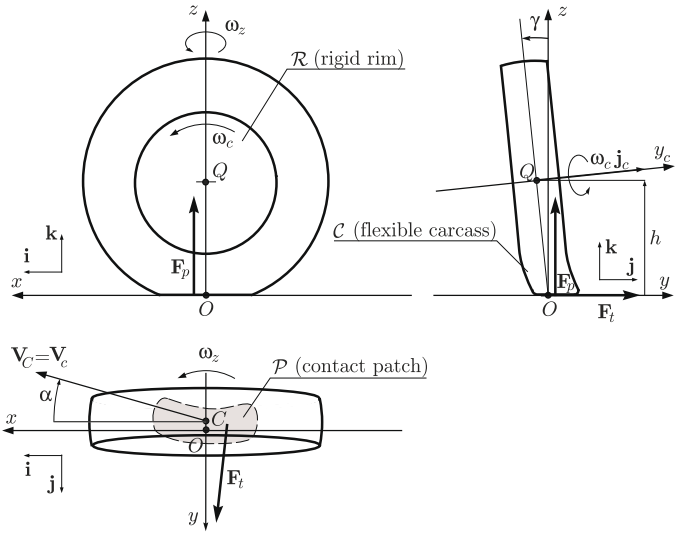

Fig. 2.2 Wheel with tire: nomenclature and reference system

An observation is in order here. The *directions* $(\mathbf{i}, \mathbf{j}, \mathbf{k})$ have a physical meaning, in the sense that they clearly mark some of the peculiar features of the rim with respect to the road. As a matter of fact, $\mathbf{k}$ is perpendicular to the road, $\mathbf{i}$ is perpendicular to both $\mathbf{k}$ and the rim axis $\mathbf{j}_c$, $\mathbf{j}$ follows accordingly. However, the *position* of the Cartesian axes (x, y, z) is arbitrary, since there is no physical reason to select a point as the origin O. This is an aspect whose implications are often underestimated.

The moving reference system $\mathsf{S} = (x, y, z; O)$ allows a more precise description of the rim kinematics. On the other hand, a reference system $\mathsf{S}_f = (x_f, y_f, z_f; O_f)$ fixed to the road is not very useful in this context.

Let $\mathbf{j}_c$ be the direction of the rim axis y_c

$$\mathbf{j}_c = \cos\gamma\,\mathbf{j} + \sin\gamma\,\mathbf{k} \tag{2.2}$$

where the *camber angle* γ of Fig. 2.2 is positive. The total *rim angular velocity* $\boldsymbol{\Omega}$ is

$$\begin{aligned}\boldsymbol{\Omega} &= \dot{\gamma}\mathbf{i} + \dot{\theta}\mathbf{j}_c + \dot{\zeta}\mathbf{k}\\ &= \dot{\gamma}\mathbf{i} + \omega_c\mathbf{j}_c + \omega_z\mathbf{k}\\ &= \dot{\gamma}\mathbf{i} + \omega_c\cos\gamma\,\mathbf{j} + (\omega_c\sin\gamma + \omega_z)\mathbf{k}\\ &= \Omega_x\mathbf{i} + \Omega_y\mathbf{j} + \Omega_z\mathbf{k}\end{aligned} \tag{2.3}$$

where $\dot{\gamma}$ is the time derivative of the camber angle, $\omega_c = \dot{\theta}$ is the angular velocity of the rim about its spindle axis, and $\omega_z = \dot{\zeta}$ is the yaw rate, that is the angular velocity of the reference system S.

It is worth noting that there are two distinct contributions to the *spin velocity* $\Omega_z \mathbf{k}$ of the rim, a camber contribution and a turn contribution[4]

$$\Omega_z = \omega_c \sin\gamma + \omega_z \tag{2.4}$$

Therefore, the same value of Ω_z can be the result of different operating conditions for the tire, depending on the amount of the camber angle γ and of the yaw rate ω_z.

By definition, the position vector OQ is (Fig. 2.2)

$$OQ = h(-\tan\gamma\,\mathbf{j} + \mathbf{k}) \tag{2.5}$$

This expression can be differentiated with respect to time to obtain

$$\begin{aligned}\mathbf{V}_Q - \mathbf{V}_O &= \dot{h}(-\tan\gamma\,\mathbf{j} + \mathbf{k}) + h\left(\omega_z \tan\gamma\,\mathbf{i} - \frac{\dot{\gamma}}{\cos^2\gamma}\mathbf{j}\right)\\ &= h\omega_z \tan\gamma\,\mathbf{i} - \left(\dot{h}\tan\gamma + h\frac{\dot{\gamma}}{\cos^2\gamma}\right)\mathbf{j} + \dot{h}\mathbf{k}\end{aligned} \tag{2.6}$$

since $\mathrm{d}\mathbf{j}/\mathrm{d}t = -\omega_z \mathbf{i}$. Even in steady-state conditions, that is $\dot{h} = \dot{\gamma} = 0$, we have $\mathbf{V}_Q = \mathbf{V}_O + h\omega_z \tan\gamma\,\mathbf{i}$ and hence the two velocities are not exactly the same, unless also $\gamma = 0$. The camber angle γ is usually very small in cars, but may be quite large in motorcycles.

The velocity of point O has, in general, longitudinal and lateral components

$$\mathbf{V}_o = \mathbf{V}_O = V_{o_x}\mathbf{i} + V_{o_y}\mathbf{j} \tag{2.7}$$

As already stated, the selection of point O is *arbitrary*, although quite reasonable. Therefore, the velocities V_{o_x} and V_{o_y} do not have much of physical meaning. A different choice for the point O would provide different values for the very same motion. However, a "wheel" is expected to have longitudinal velocities much higher than lateral ones, as will be discussed with reference to Fig. 10.23.

Summing up, the position of the rigid rim $\mathscr{R}$ with respect to the flat road is completely determined by the following six degrees of freedom:

$h(t)$ distance of point Q from the road;
$\gamma(t)$ camber angle;
$\theta(t)$ rotation of the rim about its axis y_c;
$x_f(t)$ first coordinate of point O w.r.t. S_f;
$y_f(t)$ second coordinate of point O w.r.t. S_f;
$\zeta(t)$ yaw angle of the rim.

However, owing to the circular shape of rim and the flatness of the road, the kinematics of the rigid rim $\mathscr{R}$ is also fully described by the following six functions of time:

[4] In the SAE terminology, it is $\omega_c \mathbf{j}_c$ that is called spin velocity [4, 11].

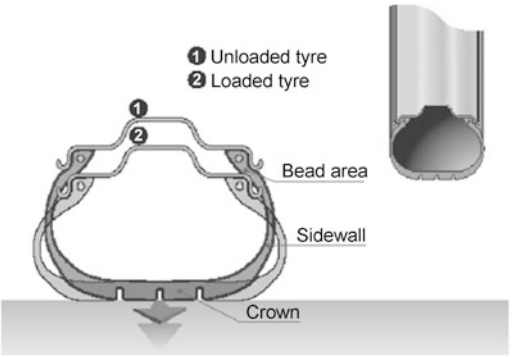

Fig. 2.3 Flexibility of the tire carcass [8]

Fig. 2.4 Structure of a radial tire [8]

$h(t)$ distance of point Q from the road;
$\gamma(t)$ camber angle;
$\omega_c(t)$ angular velocity of the rim about its axis y_c;
$V_{o_x}(t)$ longitudinal speed of O;
$V_{o_y}(t)$ lateral speed of O;
$\Omega_z(t)$ spin velocity of the rim.

The rim is in steady-state conditions if all these six quantities are constant in time. However, this is not sufficient for the wheel with tire to be in a stationary state. The flexible carcass and tire treads could still be under transient conditions.

2.3 Carcass Features

The tire carcass $\mathscr{C}$ is a highly composite and complex structure. Here we look at the tire as a vehicle component [13] and therefore it suffices to say that the inflated carcass, with its flexible sidewalls, is moderately compliant in all directions (Fig. 2.3). The external belt is also flexible, but quite inextensible (Fig. 2.4). For instance, its circumferential length is not very much affected by the vertical load

acting on the tire. The belt is covered with tread blocks whose elastic deformation and grip features highly affect the mechanical behavior of the wheel with tire [8–10].

Basically, the carcass can be seen as a nonlinear elastic structure with small hysteresis due to rate-dependent energy losses. It is assumed here that the carcass and the belt have negligible inertia, in the sense that the inertial effects are small in comparison with other causes of deformation. This is quite correct if the road is flat and the wheel motion is not "too fast".

2.4 Contact Patch

Tires are made from rubber, that is elastomeric materials to which they owe a large part of their grip capacity [17]. Grip implies contact between two surfaces: one is the tire surface and the other is the road surface.

The contact patch (or footprint) $\mathscr{P}$ is the region where the tire is in contact with the road surface. In Fig. 2.2 the contact patch is schematically shown as a single region. However, most tires have a tread pattern, with lugs and voids, and hence the contact patch is the union of many small regions (Fig. 2.5). It should be emphasized that the shape and size of the contact patch, and also its position with respect to the reference system, depend on the tire operating conditions.

Grip depends, among other things, on the *type* of road surface, its *roughness*, and whether it is *wet or not*. More precisely, grip comes basically from road roughness effects and molecular adhesion.

Road roughness effects, also known as indentation, require small bumps measuring a few microns to a few millimeters (Fig. 2.6), which dig into the surface of the rubber. On the other hand, *molecular adhesion* necessitates direct contact between the rubber and the road surface, i.e. the road must be dry.

Two main features of road surface geometry must be examined and assessed when considering tire grip, as shown in Fig. 2.6:

Macroroughness: this is the name given to the road surface texture when the distance between two consecutive rough spots is between 100 microns and 10 millimeters. This degree of roughness contributes to indentation, and to the drainage and storage of water. The load bearing surface, which depends on road macroroughness, must also be considered since it determines local pressures in the contact patch.

Microroughness: this is the name given to the road surface texture when the distance between two consecutive rough spots is between 1 and 100 microns. It is this degree of roughness which is mainly responsible for tire grip via the road roughness effects. Microroughness is related to the surface roughness of the aggregates and sands used in the composition of the road surface.

Fig. 2.5 Typical contact patch (if $\alpha = \gamma = 0$) with tread pattern

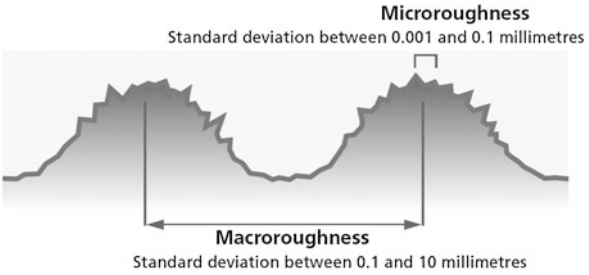

Fig. 2.6 Road roughness description [8]

2.5 Footprint Force

As well known (see, e.g., [18]), any set of forces or distributed load is statically equivalent to a force-couple system at a given (arbitrary) point O. Therefore, regardless of the degree of roughness of the road, the distributed normal and tangential loads in the footprint yield a resultant force $\mathbf{F}$ and a resultant couple vector $\mathbf{M}_O$

$$\begin{aligned} \mathbf{F} &= F_x\mathbf{i} + F_y\mathbf{j} + F_z\mathbf{k} \\ \mathbf{M}_O &= M_x\mathbf{i} + M_y\mathbf{j} + M_z\mathbf{k} \end{aligned} \tag{2.8}$$

The resultant couple $\mathbf{M}_O$ is simply the moment about the point O, but any other point could be selected. Therefore it has no particular physical meaning. However, if O is somewhere within the contact patch, the magnitude $|\mathbf{M}_O|$ is expected to be quite "small" for the wheel with tire to resemble a rigid wheel.

Traditionally, the components of $\mathbf{F}$ and $\mathbf{M}_O$ have the following names:

F_x longitudinal force;
F_y lateral force;
F_z vertical load or normal force;
M_x overturning moment;
M_y rolling resistance moment;
M_z self-aligning torque, called vertical moment here.

The names of the force components simply reaffirm their direction with respect to the chosen reference system S and hence with respect to the rim. On the other hand,

the names of the moment components, which would suggest a physical interpretation, are all quite questionable. Their values depend on the arbitrarily selected point O, and hence are arbitrary by definition.

For instance, let us discuss the name "self-aligning torque" of M_z, with reference to Fig. 2.2 and Eq. (2.10). The typical explanation for the name is that "M_z produces a restoring moment on the tire to realign the direction of travel with the direction of heading", which, more precisely, means that M_z and the slip angle α are both clockwise or both counterclockwise. But the sign and magnitude of M_z depend on the position of O, which could be anywhere! The selected origin O has nothing special, not at all. Therefore, the very same physical phenomenon, like in Fig. 2.2, may be described with O anywhere and hence by any value of M_z. The inescapable conclusion is that the name "self-aligning torque" is totally meaningless and even misleading.[5] For these reasons, here we prefer to call M_z the *vertical moment*. Similar considerations apply to M_x.

It is a classical result that any set of forces and couples in space, like $(\mathbf{F}, \mathbf{M}_O)$, is statically equivalent to a unique wrench [18]. However, in tire mechanics it is more convenient, although not mandatory, to represent the force-couple system $(\mathbf{F}, \mathbf{M}_O)$ by *two* properly located *perpendicular forces* (Fig. 2.2): a vertical force $\mathbf{F}_p = F_z\mathbf{k}$ having the line of action passing through the point with coordinates $(e_x, e_y, 0)$ such that

$$M_x = F_z e_y \quad \text{and} \quad M_y = -F_z e_x \tag{2.9}$$

and a tangential force $\mathbf{F}_t = F_x\mathbf{i} + F_y\mathbf{j}$ lying in the xy-plane and having the line of action with distance $|d_t|$ from O (properly located according to the sign of d_t)

$$M_z = \sqrt{F_x^2 + F_y^2}\, d_t = |\mathbf{F}_t| d_t \tag{2.10}$$

We remark that the two "displaced" forces $\mathbf{F}_p$ and $\mathbf{F}_t$ (Fig. 2.2) are completely equivalent to $\mathbf{F}$ and $\mathbf{M}_O$.

These forces are transferred to the rigid rim (apart for a small fraction due to the inertia and weight of the tire carcass and belt). Indeed, the equivalence of the distributed loads in the contact patch to concentrated forces and/or couples makes sense precisely because the rim is a rigid body.

For instance, the torque $\mathbf{T} = T\mathbf{j}_c$ that the distributed loads in the contact patch, and hence the force-couple system $(\mathbf{F}, \mathbf{M}_O)$, exert with respect to the wheel axis y_c is given by

$$\begin{aligned} \mathbf{T} = T\mathbf{j}_c &= \big((QO \times \mathbf{F} + \mathbf{M}_O) \cdot \mathbf{j}_c\big)\mathbf{j}_c \\ &= \left(-F_x \frac{h}{\cos\gamma} + M_y \cos\gamma + M_z \sin\gamma\right)\mathbf{j}_c \end{aligned} \tag{2.11}$$

[5] What is relevant in vehicle dynamics is the moment of $(\mathbf{F}, \mathbf{M}_O)$ with respect to the steering axis of the wheel. But this is another story.

where (2.2) and (2.5) were employed. This expression is particularly simple because the y_c-axis intersects the z-axis and is perpendicular to the x-axis (Fig. 2.2). If $\gamma = 0$, Eq. (2.11) becomes

$$T = -F_x h + M_y = -F_x h - F_z e_x \tag{2.12}$$

2.5.1 Perfectly Flat Road Surface

To perform some further mathematical investigations, it is necessary to discard completely the road roughness (Fig. 2.6) and to assume the road surface in the contact patch to be *perfectly flat*, exactly like a geometric plane (Fig. 2.2).[6] This is a fairly unrealistic assumption whose implications should not be underestimated.

Owing to the assumed flatness of the contact patch $\mathscr{P}$, we have that the *pressure* $p(x, y)\mathbf{k}$, by definition normal to the surface, is always vertical and hence forms a *parallel* distributed load. Moreover, the flatness of $\mathscr{P}$ implies that the *tangential stress* $\mathbf{t}(x, y) = t_x\mathbf{i} + t_y\mathbf{j}$ forms a *planar* distributed load. Parallel and planar distributed loads share the common feature that the resultant force and the resultant couple vector are perpendicular to each other, and therefore each force-couple system at O can be further reduced to a *single* resultant force applied along the *line of action* (in general not passing through O). A few formulae should clarify the matter.

The resultant force $\mathbf{F}_p$ and couple $\mathbf{M}_p^O$ of the distributed pressure $p(x, y)$ are given by

$$\begin{aligned} \mathbf{F}_p &= F_z\mathbf{k} = \mathbf{k}\iint_{\mathscr{P}} p(x, y)\mathrm{d}x\mathrm{d}y \\ \mathbf{M}_p^O &= M_x\mathbf{i} + M_y\mathbf{j} = \iint_{\mathscr{P}} (x\mathbf{i} + y\mathbf{j}) \times \mathbf{k}\, p(x, y)\mathrm{d}x\mathrm{d}y \end{aligned} \tag{2.13}$$

where

$$M_x = \iint_{\mathscr{P}} y p(x, y)\mathrm{d}x\mathrm{d}y = F_z e_y, \qquad M_y = -\iint_{\mathscr{P}} x p(x, y)\mathrm{d}x\mathrm{d}y = -F_z e_x \tag{2.14}$$

As expected, $\mathbf{F}_p$ and $\mathbf{M}_p^O$ are perpendicular. As shown in (2.14), the force-couple resultant $(\mathbf{F}_p, \mathbf{M}_p^O)$ can be reduced to a single force $\mathbf{F}_p$ having a vertical line of action passing through the point with coordinates $(e_x, e_y, 0)$, as shown in Fig. 2.2.

[6] More precisely, it is necessary to have a mathematical description of the shape of the road surface in the contact patch. The plane just happens to be the simplest.

The resultant tangential force $\mathbf{F}_t$ and couple $\mathbf{M}_t^O$ of the distributed tangential stress $\mathbf{t}(x, y) = t_x\mathbf{i} + t_y\mathbf{j}$ are given by

$$\begin{aligned}\mathbf{F}_t &= F_x\mathbf{i} + F_y\mathbf{j} = \iint_{\mathscr{P}} \big(t_x(x, y)\mathbf{i} + t_y(x, y)\mathbf{j}\big)\mathrm{d}x\mathrm{d}y \\ \mathbf{M}_t^O &= M_z\mathbf{k} = \iint_{\mathscr{P}} (x\mathbf{i} + y\mathbf{j}) \times (t_x\mathbf{i} + t_y\mathbf{j})\mathrm{d}x\mathrm{d}y \\ &= \mathbf{k}\iint_{\mathscr{P}} \big(xt_y(x, y) - yt_x(x, t)\big)\mathrm{d}x\mathrm{d}y = \mathbf{k}d_t\sqrt{F_x^2 + F_y^2}\end{aligned} \tag{2.15}$$

where

$$F_x = \iint_{\mathscr{P}} t_x(x, y)\mathrm{d}x\mathrm{d}y, \qquad F_y = \iint_{\mathscr{P}} t_y(x, y)\mathrm{d}x\mathrm{d}y \tag{2.16}$$

Also in this case $\mathbf{F}_t$ and $\mathbf{M}_t^O$ are perpendicular. As shown in (2.15), the force-couple resultant $(\mathbf{F}_t, \mathbf{M}_t^O)$ can be reduced to a tangential force $\mathbf{F}_t$, lying in the xy-plane and having a line of action with distance $|d_t|$ from O (properly located according to the sign of d_t), as shown in Fig. 2.2.

Obviously the more general (2.8) still holds

$$\begin{aligned}\mathbf{F} &= \mathbf{F}_p + \mathbf{F}_t \\ \mathbf{M}_O &= \mathbf{M}_p^O + \mathbf{M}_t^O\end{aligned} \tag{2.17}$$

2.6 Tire Global Mechanical Behavior

The analysis developed so far provides the tools for quite a precise description of the global mechanical behavior of a *real* wheel with tire interacting with a road. More precisely, as already stated at p. 8, we are interested in the *relationship* between the *motion* and *position* of the rim and the *force* exchanged with the road in the contact patch:

$$\text{rim kinematics} \quad \Longleftrightarrow \quad \text{force and moment}$$

We assume as given, and constant in time, both the wheel with tire (including its inflating pressure and temperature field) and the road type (including its roughness). Therefore we assume all grip features as given and constant in time.

2.6.1 Tire Transient Behavior

Knowing the mechanical behavior means knowing the relationships between the six kinematical parameters $(h, \gamma, \omega_c, V_{o_x}, V_{o_y}, \Omega_z)$ that fully characterize the position

and the motion of the rigid rim and the force-couple resultant $(\mathbf{F}, \mathbf{M}_O)$. We recall that the inertial effects of the carcass are assumed to be negligible.

Owing mostly to the flexibility of the tire structure, these relationships are of differential type, that is there exist *differential* equations

$$\begin{aligned} \mathbf{f}(\dot{\mathbf{F}}, \mathbf{F}, h, \gamma, \omega_c, V_{o_x}, V_{o_y}, \Omega_z) &= \mathbf{0} \\ \mathbf{g}(\dot{\mathbf{M}}_O, \mathbf{M}_O, h, \gamma, \omega_c, V_{o_x}, V_{o_y}, \Omega_z) &= \mathbf{0} \end{aligned} \tag{2.18}$$

In general, there might be the need of differential equations of higher order.

The identification of these differential equations by means solely of experimental tests is a formidable task. The point here is not to find them, but to appreciate that the transient behavior of a wheel with tire does indeed obey differential equations, maybe like in (2.18). Which also implies that initial conditions have to be included and the values of $(\mathbf{F}, \mathbf{M}_O)$ at time t depend on the time history.

Later on, suitable models will be developed that allow for a partial identification of (2.18) to be attempted.

2.6.2 Tire Steady-State Behavior

If all features are constant (or, at least, varying slowly) in time, the overall system is in steady-state conditions. Mathematically, it means that there exist, instead of (2.18), the following *algebraic* functions

$$\begin{aligned} \mathbf{F} &= \overline{\mathbf{F}}(h, \gamma, \omega_c, V_{o_x}, V_{o_y}, \Omega_z) \\ \mathbf{M}_O &= \overline{\mathbf{M}}_O(h, \gamma, \omega_c, V_{o_x}, V_{o_y}, \Omega_z) \end{aligned} \tag{2.19}$$

which relate the rim position and steady-state motion to the force and moment acting on the tire from the footprint. In other words, given the steady-state kinematics, we know the (constant in time) forces and couples (but not viceversa).

The algebraic functions in (2.19) are, by definition, the equilibrium states of the differential equations (2.18)

$$\begin{aligned} \mathbf{f}(\mathbf{0}, \overline{\mathbf{F}}, h, \gamma, \omega_c, V_{o_x}, V_{o_y}, \Omega_z) &= \mathbf{0} \\ \mathbf{g}(\mathbf{0}, \overline{\mathbf{M}}_O, h, \gamma, \omega_c, V_{o_x}, V_{o_y}, \Omega_z) &= \mathbf{0} \end{aligned} \tag{2.20}$$

Equations (2.19) can be split according to (2.17)

$$\begin{aligned} \mathbf{F}_p &= F_z\mathbf{k} = \overline{\mathbf{F}}_p(h, \gamma, \omega_c, V_{o_x}, V_{o_y}, \Omega_z) \\ \mathbf{F}_t &= F_x\mathbf{i} + F_y\mathbf{j} = \overline{\mathbf{F}}_t(h, \gamma, \omega_c, V_{o_x}, V_{o_y}, \Omega_z) \\ \mathbf{M}_p^O &= M_x\mathbf{i} + M_y\mathbf{j} = \overline{\mathbf{M}}_p^O(h, \gamma, \omega_c, V_{o_x}, V_{o_y}, \Omega_z) \\ \mathbf{M}_t^O &= M_z\mathbf{k} = \overline{\mathbf{M}}_t^O(h, \gamma, \omega_c, V_{o_x}, V_{o_y}, \Omega_z) \end{aligned} \tag{2.21}$$

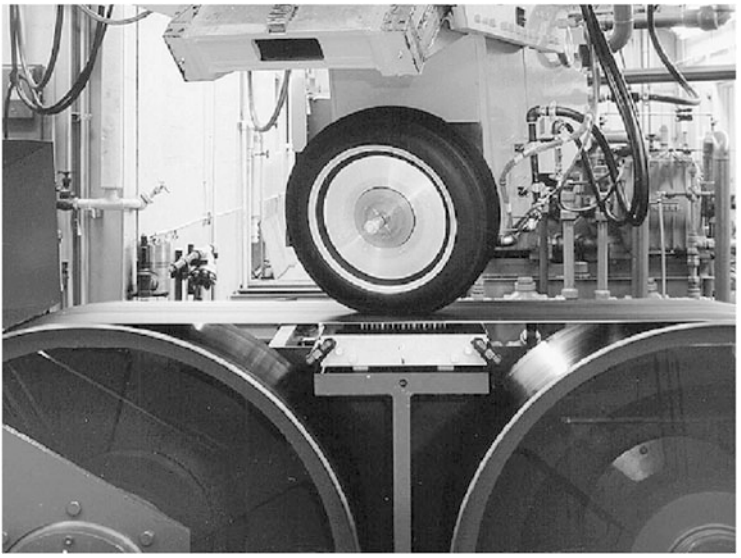

Fig. 2.7 Flat roadway testing machine (Calspan's Tire Research Facility)

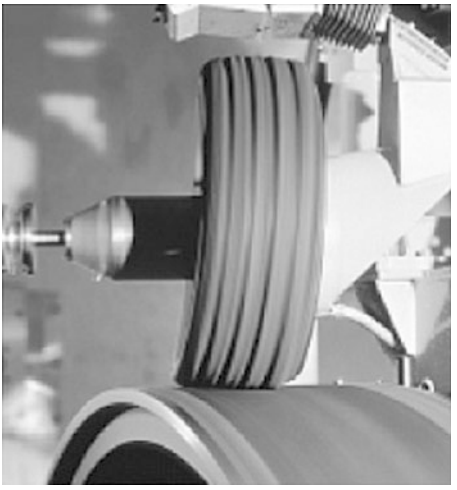

Fig. 2.8 Drum testing machine [8]

Typical *tire tests* (like in Figs. 2.7 and 2.8) aim at investigating some aspects of these functions. Actually, quite often the vertical load F_z takes the place of h as an independent variable, as discussed in Sect. 2.8. This is common practice, although it appears to be rather questionable in a neat approach to the analysis of tire mechanics. As already stated, a clearer picture arises if we follow the approach "impose the whole kinematics of the rim, measure all the forces in the contact patch" [14, p. 62].

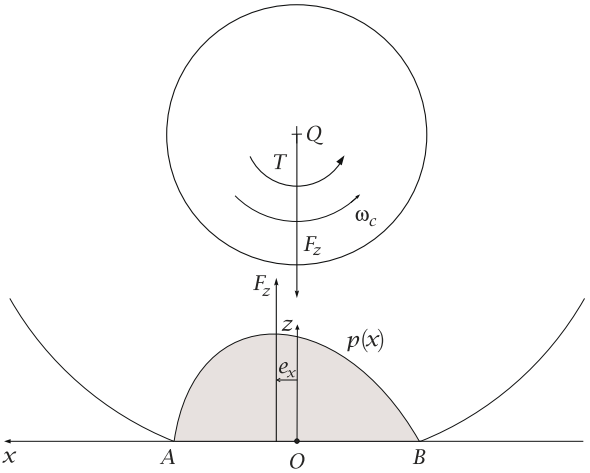

Fig. 2.9 Pure rolling: $F_x = 0$ and $T = F_z e_x$

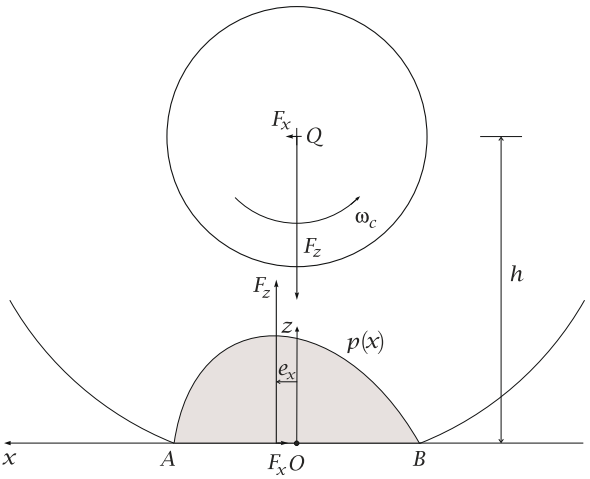

Fig. 2.10 Free rolling: $T = 0$ and $F_x h = F_z e_x$

2.6.3 Rolling Resistance

As shown schematically in Figs. 2.9 and 2.10, the rolling resistance arises because the normal pressure p in the leading half of the contact patch is higher than that in the trailing half. This is mainly caused by the hysteresis in the tire due to the deflection of the carcass while rolling. The vertical resultant $F_z\mathbf{k}$ of the pressure distribution is offset towards the front of the contact patch.

The main source of energy dissipation is therefore the visco-elasticity of the materials of which tires are made. Visco-elastic materials lose energy in the form of heat whenever they are deformed. Deformation-induced energy dissipation is the cause of about 90 % of rolling resistance [10, 19].

A number of tire operating conditions affect rolling resistance. The most important are load, inflation pressure and temperature. However, as speed increases, tire's internal temperature rises, offsetting some of the increased rolling resistance. Therefore, tire rolling resistance coefficients f are relatively constant on a relatively wide range of speeds. The values given by tire manufacturers are measured on test drums, usually at 80 km/h in accordance with ISO measurement standards.

2.6.4 Speed Independence (Almost)

Tire tests suggest that $\mathbf{F}_p$, $\mathbf{F}_t$, $\mathbf{M}_p^O$ and $\mathbf{M}_t^O$ are *almost speed independent*, if ω_c is not too high. Essentially, it means that (2.21) can be replaced by the following functions of only *five* variables:

$$\begin{aligned}
\mathbf{F}_p &= \widetilde{\mathbf{F}}_p\left(h, \gamma, \frac{V_{o_x}}{\omega_c}, \frac{V_{o_y}}{\omega_c}, \frac{\Omega_z}{\omega_c}\right) \\
\mathbf{F}_t &= \widetilde{\mathbf{F}}_t\left(h, \gamma, \frac{V_{o_x}}{\omega_c}, \frac{V_{o_y}}{\omega_c}, \frac{\Omega_z}{\omega_c}\right) \\
\mathbf{M}_p^O &= \widetilde{\mathbf{M}}_p^O\left(h, \gamma, \frac{V_{o_x}}{\omega_c}, \frac{V_{o_y}}{\omega_c}, \frac{\Omega_z}{\omega_c}\right) \\
\mathbf{M}_t^O &= \widetilde{\mathbf{M}}_t^O\left(h, \gamma, \frac{V_{o_x}}{\omega_c}, \frac{V_{o_y}}{\omega_c}, \frac{\Omega_z}{\omega_c}\right)
\end{aligned} \tag{2.22}$$

In other words, we assume that the steady-state forces and moments depend on the *geometrical* features of the rim motion (i.e., the trajectories), and not on how fast the motion develops in time. Therefore, we are discarding all inertial effects and any influence of speed on the phenomena related to grip. Of course, this may not be true at very high speeds, like in competitions.

2.6.5 Pure Rolling (not Free Rolling)

Pure rolling between two rigid surfaces that are touching at one point is a relevant topic, e.g., in robot manipulation. An in-depth discussion in the more general framework of contact kinematics can be found for instance in [12, p. 249].

Pure rolling in case of rigid bodies in *point contact* requires two kinematical conditions to be fulfilled: *no sliding* and *no mutual spin*. However, the two bodies may exchange tangential forces as far as the friction limit is not exceeded.

These concepts and results have, however, very little relevance, if any, for the (possible) definition of pure rolling of a wheel with tire. As a matter of fact, there are no rigid surfaces in contact and the footprint is certainly not a point (Fig. 2.5). Therefore, even if it is customary to speak of pure rolling of a wheel with tire, it

should be clear that it is a *totally different concept* than pure rolling between rigid bodies.

A reasonable definition of *pure rolling* for a wheel with tire, in steady-state conditions[7] and moving on a flat surface, is that the grip actions $\mathbf{t}$ have no global effect, that is

$$F_x = 0 \tag{2.23}$$

$$F_y = 0 \tag{2.24}$$

$$M_z = 0 \tag{2.25}$$

These equations do not imply that the local tangential stresses $\mathbf{t}$ in the contact patch are everywhere equal to zero, but only that their force-couple resultant is zero (cf. (2.15)). Therefore, the road applies to the wheel only a vertical force $\mathbf{F}_p = F_z\mathbf{k}$ and a horizontal moment $\mathbf{M}_p^O = M_x\mathbf{i} + M_y\mathbf{j}$.

The goal now is to find the kinematical conditions to be imposed to the rim to fulfill Eqs. (2.23)–(2.25). In general, the six parameters in Eq. (2.21) should be considered. However, it is more common to assume that *five* parameters suffice, like in (2.22) (as already discussed, it is less general, but simpler)

$$\widetilde{F}_x\left(h, \gamma, \frac{V_{ox}}{\omega_c}, \frac{V_{oy}}{\omega_c}, \frac{\Omega_z}{\omega_c}\right) = 0 \tag{2.26}$$

$$\widetilde{F}_y\left(h, \gamma, \frac{V_{ox}}{\omega_c}, \frac{V_{oy}}{\omega_c}, \frac{\Omega_z}{\omega_c}\right) = 0 \tag{2.27}$$

$$\widetilde{M}_z\left(h, \gamma, \frac{V_{ox}}{\omega_c}, \frac{V_{oy}}{\omega_c}, \frac{\Omega_z}{\omega_c}\right) = 0 \tag{2.28}$$

It is worth noting that *pure rolling* and *free rolling* are not the same concept [14, p. 65]. They provide different ways to balance the rolling resistance moment $M_y = -F_z e_x$. According to (2.12), we have pure rolling if $F_x = 0$ (Fig. 2.9), while free rolling means $T = 0$ (Fig. 2.10). However, the ratio $f = e_x/h$, called the *rolling resistance coefficient*, is typically less than 0.015 for car tires and hence there is not much quantitative difference between pure and free rolling.

2.6.5.1 Zero Longitudinal Force

First, let us consider Eq. (2.26) alone

$$\widetilde{F}_x\left(h, \gamma, \frac{V_{ox}}{\omega_c}, \frac{V_{oy}}{\omega_c}, \frac{\Omega_z}{\omega_c}\right) = 0 \tag{2.29}$$

[7] We have basically a steady-state behavior even if the operating conditions do not change "too fast".

which means that $F_x = 0$ if

$$\frac{V_{o_x}}{\omega_c} = f_x\left(h, \gamma, \frac{V_{o_y}}{\omega_c}, \frac{\Omega_z}{\omega_c}\right) \tag{2.30}$$

Under many circumstances there is experimental evidence that the relation above almost does not depend on V_{o_y} and can be recast in the following more explicit form[8]

$$\frac{V_{o_x}}{\omega_c} = r_r(h, \gamma) + \frac{\omega_z}{\omega_c} c_r(h, \gamma) \tag{2.31}$$

that is

$$V_{o_x} = \omega_c r_r(h, \gamma) + \omega_z c_r(h, \gamma) \tag{2.32}$$

This equation strongly suggests to take into account a *special point* C on the y-axis such that (Fig. 2.11 and also Fig. 2.2)

$$OC = c_r(h, \gamma)\mathbf{j} \tag{2.33}$$

where c_r is a (short) signed length. Point C would be the point of contact in case of a rigid wheel. Quite often point O and C have almost the same velocity, although their distance c_r may not be negligible (Fig. 2.11).

Equation (2.31) can be rearranged to get

$$\frac{V_{o_x} - \omega_z c_r(h, \gamma)}{\omega_c} = \frac{V_{c_x}}{\omega_c} = r_r(h, \gamma) \tag{2.34}$$

This is quite a remarkable result and clarifies the role of point C: the condition $F_x = 0$ requires $V_{c_x} = \omega_c r_r(h, \gamma)$, regardless of the value of ω_z (and also of V_{o_y}).

The function $r_r(h, \gamma)$ can be seen as a sort of longitudinal *pure rolling radius* [19, p. 18], although this name would be really meaningful only for a rigid wheel. Actually, rolling or sliding do not change the radius of a rigid wheel. As already stated, a wheel with tire has little to share with a rigid wheel.

The value of $r_r(h, \gamma)$ for given (h, γ) can be obtained by means of the usual indoor testing machines (Figs. 2.7 and 2.8) with $\omega_z = 0$. An additional, more difficult, test with $\omega_z \neq 0$ is required to obtain also $c_r(h, \gamma)$ and hence the position of C with respect to O. Car tires operate at low values of γ and hence have almost constant r_r.

In general, we can choose the origin O of the reference system to coincide with C when $\gamma = 0$. Therefore, only for large values of the camber angle, that is for motorcycle tires, the distance $|c_r|$ can reach a few centimeters (Fig. 2.11).

A rough estimate shows that the ratio $|\omega_z/\omega_c|$ is typically very small, ranging from zero (straight running) up to about 0.01. It follows that quite often $|(\omega_z/\omega_c)c_r|$

[8] However, in the brush model, and precisely at p. 294, the effect of the elastic compliance of the carcass on C is taken into account.

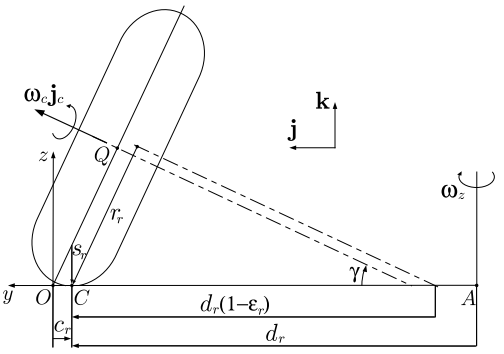

Fig. 2.11 Pure rolling of a cambered wheel

may be negligible and points O and C have almost the same velocity. However, particularly in competitions, it could be worthwhile to have a more detailed characterization of the behavior of the tire which takes into account even these minor aspects.

2.6.5.2 Zero Lateral Force

We can now discuss when the lateral force and the vertical moment are equal to zero.

According to (2.27), we have that $F_y = 0$ if

$$\widetilde{F}_y\left(h, \gamma, \frac{V_{ox}}{\omega_c}, \frac{V_{oy}}{\omega_c}, \frac{\Omega_z}{\omega_c}\right) = 0 \tag{2.35}$$

which means

$$\frac{V_{c_y}}{\omega_c} = f_y\left(h, \gamma, \frac{\Omega_z}{\omega_c}\right) \tag{2.36}$$

where, as suggested by the experimental tests, there is no dependence on the value of V_{c_x}. For convenience, the lateral velocity V_{c_y} of point C has been employed, instead of that of point O (Fig. 2.11). Nevertheless, it seems that (2.36) does not have a simple structure like (2.34).

2.6.5.3 Zero Vertical Moment

Like in (2.28), the vertical moment with respect to O is zero, that is $M_z = 0$ if

$$\widetilde{M}_z\left(h, \gamma, \frac{V_{ox}}{\omega_c}, \frac{V_{oy}}{\omega_c}, \frac{\Omega_z}{\omega_c}\right) = 0 \tag{2.37}$$

which provides

$$\frac{V_{c_y}}{\omega_c} = f_z\left(h, \gamma, \frac{\Omega_z}{\omega_c}\right) \tag{2.38}$$

where, like in (2.36), there is no dependence on the value of V_{c_x}. Also in this case, it is not possible to be more specific about the structure of this equation.

2.6.5.4 Zero Lateral Force and Vertical Moment

However, the fulfilment of *both* conditions (2.36) and (2.38) together, that is $F_y = 0$ and $M_z = 0$, yields these noteworthy results

$$V_{c_y} = \dot{\gamma} s_r(h, \gamma) \tag{2.39}$$

$$\Omega_z = \omega_c \sin\gamma \varepsilon_r(h, \gamma) \tag{2.40}$$

which have a simple structure. To have almost steady-state conditions, it has to be $|\dot{\gamma}| \ll \omega_c$, which is almost always the case. Indeed, in a wheel we do normally expect $|V_{c_x}| \gg |V_{c_y}|$ (Fig. 2.11).

The function $s_r(h, \gamma)$ is a sort of lateral pure rolling radius. It is significant in large motorcycle tires with toroidal shape (i.e., circular section with almost constant radius s_r).[9]

Sometimes $\varepsilon_r(h, \gamma)$ is called the *camber reduction factor* [14, p. 119], [15]. A car tire may have $0.4 < \varepsilon_r < 0.6$, while a motorcycle tire has ε_r almost equal to 0. The term $\sin\gamma$ in the r.h.s. of (2.40) simply states that the spin velocity Ω_z must be zero to have pure rolling with $\gamma = 0$.

Since $\Omega_z = \omega_z + \omega_c \sin\gamma$ (cf. (2.4)), Eq. (2.40) is equivalent to

$$\frac{\omega_z}{\omega_c} = -\sin\gamma\big(1 - \varepsilon_r(h, \gamma)\big) \tag{2.41}$$

Therefore, to have $F_y = 0$ and $M_z = 0$, a cambered wheel with tire must go round as shown in Fig. 2.12, with a suitable combination of ω_c and ω_z. Since no condition is set by (2.41) on the longitudinal velocity V_{c_x}, the radius of the circular path traced on the road by point C does not matter.

[9] In a toroidal *rigid* wheel with maximum radius r_0 and lateral radius s_r we would have $r_r = r_0 - s_r(1 - \cos\gamma)$, $c_r = -\tan\gamma s_r$ and $\varepsilon_r = 0$. It follows that $\dot{c}_r \neq -\dot{\gamma} s_r$.

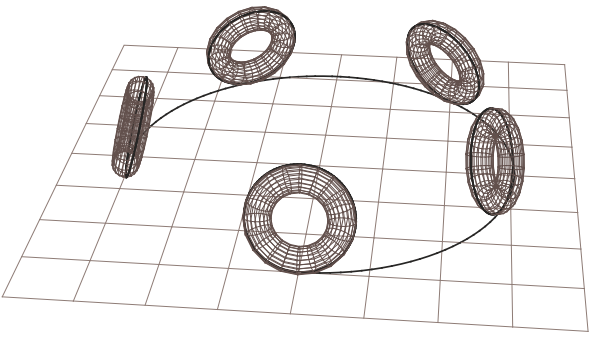

Fig. 2.12 Cambered toroidal wheel moving on a circular path (courtesy of M. Gabiccini)

2.7 Tire Slips

Summing up, we have obtained the following kinematic conditions for a wheel with tire to be in what we have defined *pure rolling* in (2.23)–(2.25):

$$
\begin{aligned}
F_x = 0 \quad &\Longleftrightarrow \quad \frac{V_{c_x}}{\omega_c} = r_r(h,\gamma) \\
\begin{cases} F_y = 0 \\ M_z = 0 \end{cases} \quad &\Longleftrightarrow \quad \begin{cases} \dfrac{V_{c_y}}{\omega_c} = \dfrac{\dot{\gamma}}{\omega_c} s_r(h,\gamma) \\ \dfrac{\Omega_z}{\omega_c} = \sin\gamma\, \varepsilon_r(h,\gamma) \end{cases}
\end{aligned}
\tag{2.42}
$$

with $OC = c_r(h,\gamma)\mathbf{j}$ (Fig. 2.11).

These equations provide a sort of *reference condition* for the behavior of a wheel with tire. Moreover, they are of key relevance for the subsequent definition of *tire slips*.

The fulfillment of only the first condition in (2.42) corresponds to longitudinal pure rolling.

It is worth recalling the main assumptions made (which are not always verified in real life):

- negligible inertial effects (five instead of six parameters);
- grip features unaffected by speed;
- point C not affected by ω_z;
- lateral velocity not affecting $F_x = 0$;
- longitudinal velocity not affecting $F_y = 0$ and $M_z = 0$.

2.7.1 Rolling Velocity

Point C and the first two equations in (2.42) provide the basis for the definition of the so-called *rolling velocity* $\mathbf{V}_r$ (Fig. 2.11)

$$\begin{aligned}\mathbf{V}_r &= \omega_c r_r(h,\gamma)\mathbf{i} + \dot{\gamma} s_r(h,\gamma)\mathbf{j} \\ &\approx \omega_c r_r \mathbf{i} = V_r \mathbf{i}\end{aligned} \tag{2.43}$$

Similarly, the third equation in (2.42) leads to the definition of the *rolling spin velocity* Ω_r

$$\Omega_r = \omega_c \sin\gamma\, \varepsilon_r(h,\gamma) \tag{2.44}$$

Therefore, for a wheel with tire to be in pure rolling it is necessary (according to (2.42)) that

$$\mathbf{V}_c = \mathbf{V}_r \quad \text{and} \quad \Omega_z = \Omega_r \tag{2.45}$$

To fulfill these conditions, in the case $\dot{\gamma} = 0$, we must move the wheel on a circular path centered at A (Figs. 2.12 and 2.11), with radius $AC = d_r(h,\gamma)\mathbf{j}$ such that

$$V_{c_x} = V_r = \omega_c r_r = -\omega_z d_r = \omega_c \sin\gamma\,(1-\varepsilon_r) d_r \tag{2.46}$$

which yields

$$d_r = \frac{r_r}{(1-\varepsilon_r)\sin\gamma} \tag{2.47}$$

Typically the rolling radius r_r is slightly bigger than the distance of point C from the rim axis (Fig. 2.11).

It is often stated that "a free-rolling tire with a camber angle would move on a circular path". This statement is clearly incorrect. It should be reformulated as "a tire with camber must be moved on a definite circular path to have pure/free rolling" (Fig. 2.12). We are not doing dynamics here, but only investigating the (almost) steady-state behavior of wheels with tire. Therefore, we can say nothing about what a wheel would do by itself.

2.7.2 Definition of Tire Slips

Let us consider a wheel with tire under real operating conditions, that is *not* necessarily in pure rolling. The velocity of point C (defined in (2.33)) is called the *speed of travel* $\mathbf{V}_c$ of the wheel (Fig. 2.11)

$$\mathbf{V}_c = V_{c_x}\mathbf{i} + V_{c_y}\mathbf{j} = (V_{o_x} - \omega_z c_r)\mathbf{i} + (V_{o_y} + \dot{c}_r)\mathbf{j} \tag{2.48}$$

The components of $\mathbf{V}_c$ also have specific names: V_{c_x} is the *forward velocity* and V_{c_y} is the *lateral velocity*.

To describe any steady-state conditions of a wheel with tire we need at least two parameters plus three kinematical quantities, as in (2.22). However, it is more informative to say how "distant" these three quantities are from pure rolling. It is therefore convenient to define the *slip velocity* $\mathbf{V}_s$ [16]

$$\mathbf{V}_s = \mathbf{V}_c - \mathbf{V}_r \tag{2.49}$$

as the difference between the speed of travel and the rolling velocity (2.43). Similarly, it is useful to define what can be called the *slip spin velocity* Ω_{s_z}

$$\begin{aligned} \Omega_{s_z} &= \Omega_z - \Omega_r \\ &= \Omega_z - \omega_c \sin\gamma\, \varepsilon_r(h,\gamma) \\ &= (\omega_z + \omega_c \sin\gamma) - \omega_c \sin\gamma\, \varepsilon_r \\ &= \omega_z + \omega_c \sin\gamma\,(1-\varepsilon_r) \end{aligned} \tag{2.50}$$

As already discussed, *the complete characterization of pure rolling conditions essentially means obtaining the following four functions* (Fig. 2.11)

$$c_r(h,\gamma), \qquad r_r(h,\gamma), \qquad s_r(h,\gamma), \qquad \varepsilon_r(h,\gamma) \tag{2.51}$$

Of them, the rolling radius r_r is the most important, followed by the camber reduction factor ε_r.

Once the pure rolling experimental investigation has been carried out, it is possible, and even advisable, to perform some simple changes of parameters based on (2.42), (2.49) and (2.50), which lead to the definition of the well known (wheel with) tire *slips* σ_x, σ_y and φ:

$$r_r(h,\gamma)\sigma_x = \frac{V_{c_x}}{\omega_c} - r_r(h,\gamma) = \frac{V_{s_x}}{\omega_c} \tag{2.52}$$

$$r_r(h,\gamma)\sigma_y = \frac{V_{c_y}}{\omega_c} - \frac{\dot\gamma}{\omega_c} s_r(h,\gamma) = \frac{V_{s_y}}{\omega_c} \tag{2.53}$$

$$r_r(h,\gamma)\varphi = -\left(\frac{\Omega_z}{\omega_c} - \sin\gamma\, \varepsilon_r(h,\gamma)\right) = \frac{\Omega_{s_z}}{\omega_c} \tag{2.54}$$

that is

$$\sigma_x = \frac{V_{c_x} - \omega_c r_r}{\omega_c r_r} = \frac{(V_{o_x} - \omega_z c_r(h,\gamma)) - \omega_c r_r(h,\gamma)}{\omega_c r_r(h,\gamma)} = \frac{V_{c_x}}{V_r} - 1 = \frac{V_{s_x}}{V_r} \tag{2.55}$$

$$\sigma_y = \frac{V_{c_y} - \dot\gamma s_r}{\omega_c r_r} = \frac{(V_{o_y} + \dot c_r(h,\gamma)) - \dot\gamma s_r(h,\gamma)}{\omega_c r_r(h,\gamma)} = -\frac{V_{c_x}\tan\alpha}{V_r} = \frac{V_{s_y}}{V_r} \tag{2.56}$$

$$\varphi = -\frac{\Omega_z - \omega_c \sin\gamma\, \varepsilon_r}{\omega_c r_r} = -\frac{\omega_z + \omega_c \sin\gamma(1-\varepsilon_r(h,\gamma))}{\omega_c r_r(h,\gamma)} = -\frac{\Omega_{s_z}}{V_r} \tag{2.57}$$

These quantities have the following names [14, 15]:

σ_x theoretical longitudinal slip ($\sigma_x > 0$ means breaking);
σ_y theoretical lateral slip;
φ spin slip.

The first two can be thought of as the components of the (*translational*) *theoretical slip* $\boldsymbol{\sigma}$

$$\boldsymbol{\sigma} = \sigma_x \mathbf{i} + \sigma_y \mathbf{j} = \frac{\mathbf{V}_c - \mathbf{V}_r}{V_r} = \frac{\mathbf{V}_s}{V_r} \tag{2.58}$$

while

$$\varphi = -\frac{\Omega_z - \Omega_r}{V_r} = -\frac{\Omega_{s_z}}{V_r} \tag{2.59}$$

The longitudinal and lateral slips are dimensionless, whereas the spin slip is not: $[\varphi] = \mathrm{m}^{-1}$.

Quite often tire tests are conducted with $\omega_z = 0$. In that case, the spin slip simply becomes

$$\varphi = -\frac{\sin\gamma\,(1 - \varepsilon_r(h, \gamma))}{r_r(h, \gamma)} \tag{2.60}$$

On the other hand, if there is only the yaw rate contribution (i.e., $\gamma = 0$) it is customary to speak of *turn slip* φ_t

$$\varphi_t = -\frac{\omega_z}{V_r} \tag{2.61}$$

Summing up, the *pure rolling* conditions (2.42) are therefore equivalent to

$$\begin{cases} \sigma_x = 0 \\ \sigma_y = 0 \\ \varphi = 0 \end{cases} \tag{2.62}$$

which look simpler, but are useless without the availability of r_r, c_r, s_r and ε_r in (2.51).

The theoretical slips could be defined with reference to point O instead of C (Fig. 2.11). In that case, according to (2.48), the correct definitions are

$$\sigma_x = \frac{(V_{o_x} - \omega_z c_r) - \omega_c r_r}{\omega_c r_r}, \qquad \sigma_y = \frac{(V_{o_y} + \dot{c}_r) - \dot{\gamma} s_r}{\omega_c r_r} \tag{2.63}$$

Although, as will be shown, the theoretical slip $\boldsymbol{\sigma}$ is a better way to describe the tire behavior, it is common practice to use the components of the *practical slip* $\boldsymbol{\kappa}$ instead

$$\kappa_x = \left(\frac{\omega_c r_r}{V_{c_x}}\right)\sigma_x = \frac{1}{1 + \sigma_x}\sigma_x = \frac{V_{c_x} - \omega_c r_r}{V_{c_x}} \tag{2.64}$$

$$\kappa_y = \left(\frac{\omega_c r_r}{V_{c_x}}\right)\sigma_y = \frac{1}{1 + \sigma_x}\sigma_y = -\tan\alpha \approx -\alpha \tag{2.65}$$

or, conversely

$$\sigma_x = \frac{1}{1-\kappa_x}\kappa_x = \kappa_x\left(1+\kappa_x+O\left(\kappa_x^2\right)\right) \tag{2.66}$$

$$\sigma_y = \frac{1}{1-\kappa_x}\kappa_y = \kappa_y\left(1+\kappa_x+O\left(\kappa_x^2\right)\right) \tag{2.67}$$

which also shows that practical and theoretical slips are almost equal only when the longitudinal slip is small.

The practical slip is only apparently simpler and its use should be discouraged. The *slip ratio* $\kappa = -\kappa_x$ is also often employed, along with the slip angle $\alpha \approx -\kappa_y$. The approximation is quite good because the slip angle normally does not exceed 15°, that is 0.26 rad.

As discussed in [11, p. 39] and also in [14, p. 597], a number of slip ratio definitions are used worldwide [1, 4–6, 19]. A check, particularly of the sign conventions, is therefore advisable. This can be easily done for some typical conditions like locked wheel ($\omega_c = 0$), or spinning wheel ($\omega_c = \infty$). For instance, with the definitions given here we have $\sigma_x = +\infty$, $\kappa_x = 1$ and $\kappa = -1$ for a traveling locked wheel.

It is worth remarking that *all these slip quantities are just a way to describe the motion of the rigid wheel rim, not of the tire*. Therefore they do not provide any direct information on the amount of sliding at any point of the contact patch. In this regard their names may be misleading. More precisely, *sliding* or *adhesion* is a *local* property of any point in the contact patch, whereas *slip* is a *global* property of the rim motion. They are completely different concepts.

2.7.3 Slip Angle

The *slip angle* α is defined as the angle between the rolling velocity $\mathbf{V}_r$ and the speed of travel $\mathbf{V}_c$. However, according to (2.48) and (2.43), when $\dot{\gamma} \approx 0$ it is almost equal to the angle between $\mathbf{i}$ and $\mathbf{V}_c$ (Fig. 2.2)[10]

$$\tan\alpha = -\frac{V_{c_y}}{V_{c_x}} \tag{2.68}$$

that is $V_{c_y} = -V_{c_x}\tan\alpha$. For convenience, α is *positive* when measured *clockwise*, that is when it is like in Fig. 2.2.[11]

Of course, a non-sliding rigid wheel has a slip angle constantly equal to zero. On the other hand, a tire may very well exhibit slip angles. However, as will be shown,

[10] Common definitions of the slip angle, like "α being the difference in wheel heading and direction" are not sufficiently precise.

[11] All other angles are positive angles if measured counterclockwise, as usually done in mathematical writing.

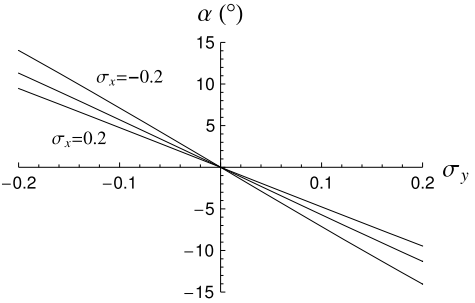

Fig. 2.13 Slip angle α as a function of σ_x and σ_y

a wheel with tire can exchange with the road very high longitudinal and lateral forces still with *small* slip angles (as shown in the important Fig. 10.23). This is one of the reasons that makes a wheel with tire behave quite close to a wheel, indeed.

More precisely, (2.68) can be rewritten as

$$\tan\alpha = -\frac{\sigma_y}{1+\sigma_x} = -\frac{\sigma_y}{\sigma_x}\left(\frac{\sigma}{\sigma+\sqrt{1+(\sigma_y/\sigma_x)^2}}\right) \tag{2.69}$$

which means that the slip angle is in the range $\pm 10 \circ$ if $\sigma < 0.2$, as shown in Fig. 2.13. This is why real tires are built in such a way to provide the best performances with values of σ below 0.2, as will also be discussed later on with reference to Fig. 10.23.

2.8 Grip Forces and Tire Slips

In (2.21) it was suggested that the steady-state global mechanical behavior of a wheel with tire could be described by means of forces and moments depending on (h, γ) to identify the rim position, and on other four kinematical parameters to determine the rim motion. We have shown that, by defining the *pure rolling* conditions and the *tire slips*, it is often possible to obtain a satisfactory description of the global mechanical behavior by means of only *three* kinematical parameters $(\sigma_x, \sigma_y, \varphi)$

$$\begin{aligned} F_x &= \widehat{F}_x(h, \gamma, \sigma_x, \sigma_y, \varphi) \\ F_y &= \widehat{F}_y(h, \gamma, \sigma_x, \sigma_y, \varphi) \\ M_z &= \widehat{M}_z(h, \gamma, \sigma_x, \sigma_y, \varphi) \end{aligned} \tag{2.70}$$

Instead of the vertical height h, it is customary to employ the vertical load F_z as an input variable. This can be safely done since

$$h = h(F_z, \gamma) \tag{2.71}$$

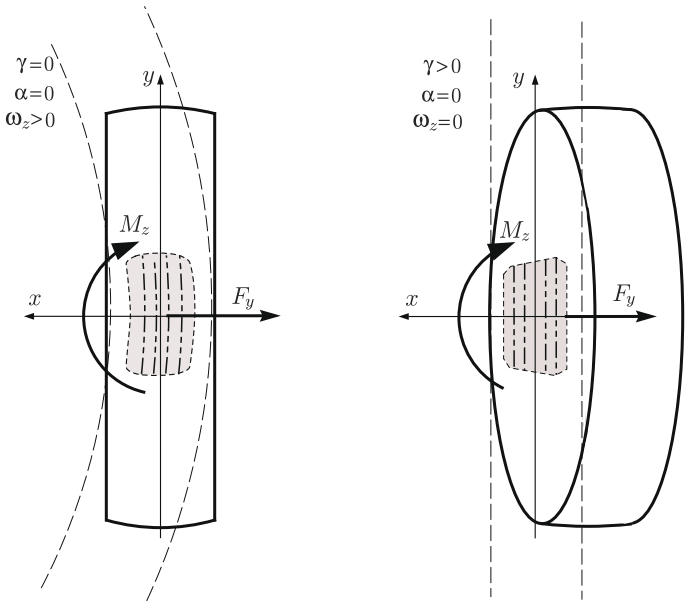

Fig. 2.14 Two different operating conditions, but with the same spin slip φ

with very little influence by the other parameters (cf. (2.21)). Therefore, the (almost) steady-state global mechanical behavior of a wheel with tire moving not too fast on a flat road is conveniently described by the following functions

$$\begin{aligned} F_x &= F_x(F_z, \gamma, \sigma_x, \sigma_y, \varphi) \\ F_y &= F_y(F_z, \gamma, \sigma_x, \sigma_y, \varphi) \\ M_z &= M_z(F_z, \gamma, \sigma_x, \sigma_y, \varphi) \end{aligned} \tag{2.72}$$

Similarly, (2.51) can be recast as

$$c_r = c_r(F_z, \gamma), \qquad r_r = r_r(F_z, \gamma), \qquad s_r = s_r(F_z, \gamma), \qquad \varepsilon_r = \varepsilon_r(F_z, \gamma) \tag{2.73}$$

It is often overlooked that F_x, F_y and M_z (Eqs. (2.70) and (2.72)) depend on *both* the camber angle γ and the spin slip φ. In other words, two operating conditions with the same φ, but obtained with different γ's, do not provide the same values of F_x, F_y and M_z, even if F_z, σ_x and σ_y are the same. For instance, the same value of φ can be obtained with no camber γ and positive yaw rate ω_z or with positive γ and no ω_z, as shown in Fig. 2.14. The two contact patches are certainly not equal to each other, and so the forces and moments. The same value of φ means that the rim has the same motion, but not the same position, if γ is different.

We remind that the moment M_z in (2.72) is with respect to a vertical axis passing through a point O chosen in quite an arbitrary way. Therefore, any attempt to attach a physical interpretation to M_z must take care of the position selected for O.

Unfortunately, it is common practice to employ the following functions, instead of (2.72)

$$\begin{aligned} F_x &= F_x^p(F_z, \gamma, \kappa_x, \alpha, \omega_z) \\ F_y &= F_y^p(F_z, \gamma, \kappa_x, \alpha, \omega_z) \\ M_z &= M_z^p(F_z, \gamma, \kappa_x, \alpha, \omega_z) \end{aligned} \tag{2.74}$$

They are, in principle, equivalent to (2.72). However, using the longitudinal practical slip κ_x, the slip angle α and the yaw rate ω_z provides a less systematic description of the tire mechanical behavior. It looks simpler, but ultimately it is not.

2.9 Tire Testing

Tire testing aims at the full identification of the three functions (2.72) or (2.74), that is of the *relationship* between the *motion* and *position* of the rim and the *force* and *moment* exchanged with the road in the contact patch

$$\text{rim kinematics} \quad \Longleftrightarrow \quad \text{force and moment}$$

Actually, this goal had already been stated in Sect. 2.1. The difference is that now we have defined the tire slips, that is a precise set of parameters to control the rim kinematics.

Indoor tire testing facilities (Figs. 2.7 and 2.8) usually have $\omega_z = 0$ in steady-state tests, and hence lack in generality by imposing a link between γ and φ (cf. (2.60)). However, in most practical applications in road vehicles we have $|\omega_z/\omega_c| < 0.01$ and ω_z can indeed be neglected.[12]

Owing to (2.42) and (2.62), it is meaningful to perform experimental tests for the so-called *pure slip conditions*. Basically it means setting $\gamma = \varphi = 0$ and either $\sigma_y = 0$ or $\sigma_x = 0$. In the first case we have pure longitudinal slip and hence only the longitudinal force $F_x = F_x(F_z, 0, \sigma_x, 0, 0)$, which is a very special case of (2.72). In the second case we have pure lateral slip, which allows for the experimental identification of the functions $F_y = F_y(F_z, 0, 0, \sigma_y, 0)$ and $M_z = M_z(F_z, 0, 0, \sigma_y, 0)$, which are also very special cases.

Unfortunately, the practical longitudinal slip κ_x and the slip angle α usually take the place of σ_x and σ_y, respectively [2].

[12] In a step steer the steering wheel of a car may reach $\omega_z = 20°/\text{s} = 0.35$ rad/s. At a forward speed of 20 m/s, the same wheels have about $\omega_c = 80$ rad/s. The contribution of ω_z to φ is therefore like a camber angle $\gamma \approx 0.5°$.

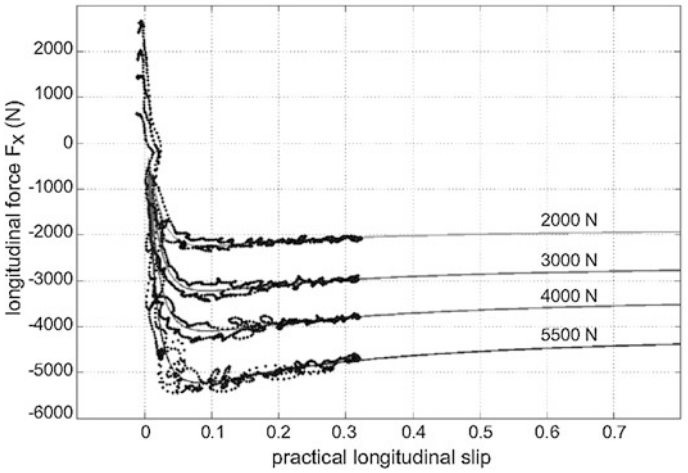

Fig. 2.15 Experimental results: longitudinal force F_x vs practical longitudinal slip κ_x for four values of the vertical load F_z

2.9.1 Pure Longitudinal Slip

Figure 2.15 shows the typical behavior of the longitudinal force F_x as a function of the practical longitudinal slip κ_x under pure braking conditions, for several values of the vertical load F_z. More precisely, it is the plot of $F_x^p(F_z, 0, \kappa_x, 0, 0)$. It is very important to note that:

- the maximum absolute value of F_x (i.e., the peak value $F_x^{\max}$) was obtained for $\kappa_x \approx 0.1$ (i.e., $\sigma_x = 0.11$);
- F_x grows *less than proportionally* with respect to the vertical load.

Both these aspects of tire behavior have great relevance in vehicle dynamics.

Also quite relevant are the values of the *longitudinal slip stiffness* C_{κ_x}, that is minus the slope of each curve at zero slip

$$C_{\kappa_x}(F_z) = -\left.\frac{\partial F_x^p}{\partial \kappa_x}\right|_{\kappa_x=0} \tag{2.75}$$

and the *global longitudinal friction coefficient* μ_p^x, that is the ratio between the peak value $F_x^{\max} = \max(|F_x^p|)$ and the corresponding vertical load

$$\mu_p^x(F_z) = \frac{F_x^{\max}}{F_z} \tag{2.76}$$

Typically, as shown in Fig. 2.16, it slightly decreases as the vertical load grows.

On the practical side, it is of some interest to observe that

- the experimental values are affected by significant errors;

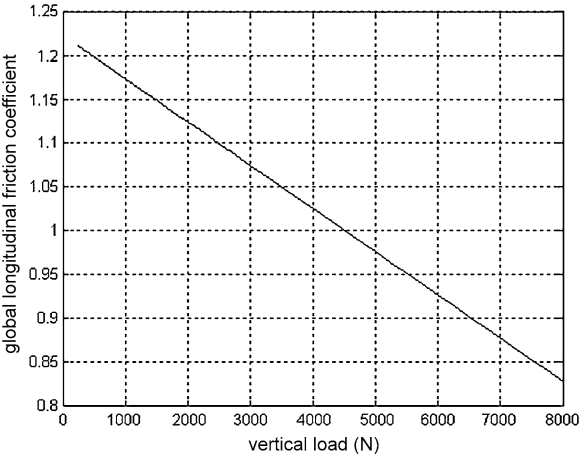

Fig. 2.16 Global longitudinal friction coefficient μ_p^x vs vertical load F_z

- the tests were carried out till $\kappa_x \approx 0.3$, to avoid wheel locking and excessive damage to the tire tread;
- the offset of F_x for $\kappa_x = 0$ is due to the rolling resistance: the wheel was (erroneously, but typically) under free rolling conditions, not pure rolling.

2.9.2 Pure Lateral Slip

Figure 2.17 shows the typical behavior of the lateral force F_y as a function of the slip angle α, for three values of F_z. More precisely, it is the plot of $F_y^p(F_z, 0, 0, \alpha, 0)$. It is very important to note that

- the maximum absolute value of F_y (i.e., the peak value $F_y^{\max}$) was obtained for $\alpha \approx \pm 8°$ (i.e., $\tan\alpha = -\sigma_y = \pm 0.14$);
- F_y grows *less than proportionally* with respect to the vertical load.

Also quite relevant are the values of the *lateral slip stiffness* C_α, also called *cornering stiffness*

$$C_\alpha(F_z) = \left.\frac{\partial F_y^p}{\partial \alpha}\right|_{\alpha=0} \tag{2.77}$$

that is the slope at the origin. As shown in Fig. 2.18, C_α grows less than proportionally with F_z, and actually it can even decrease at exceedingly high values of the vertical load.

Another important quantity is the *global lateral friction coefficient* μ_p^y, that is the ratio between the peak value $F_y^{\max} = \max(|F_y^p|)$ and the vertical load

$$\mu_p^y(F_z) = \frac{F_y^{\max}}{F_z} \tag{2.78}$$

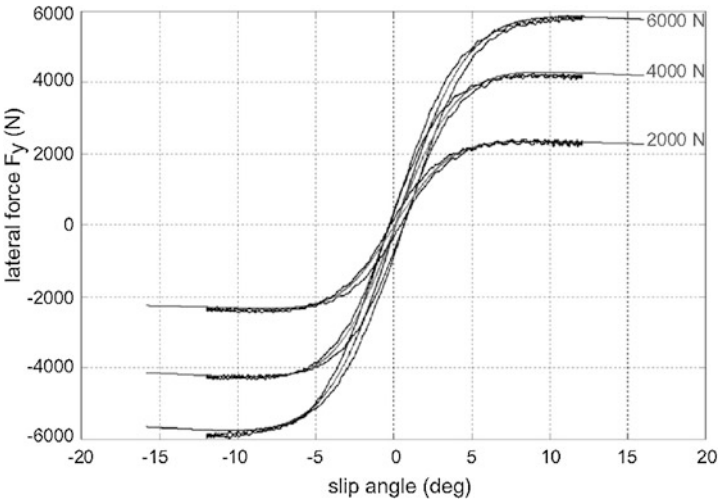

Fig. 2.17 Experimental results: lateral force F_y vs slip angle α for three values of the vertical load F_z

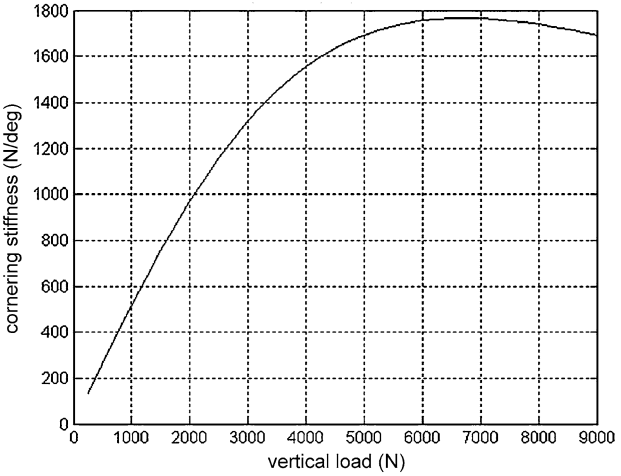

Fig. 2.18 Cornering stiffness C_α vs vertical load F_z

As shown in Fig. 2.19, it slightly decreases with F_z.

Comparing Figs. 2.16 and 2.19 we see that similar peak values for F_x and F_y are obtained for the same vertical load, that is $\mu_p^x \approx \mu_p^y$. Typically, μ_p^x is slightly greater than μ_p^y.

On the practical side it is to note that

- the experimental values are affected by small errors;
- the tests were carried out till $\alpha \approx 12°$, to avoid damaging the tire tread.

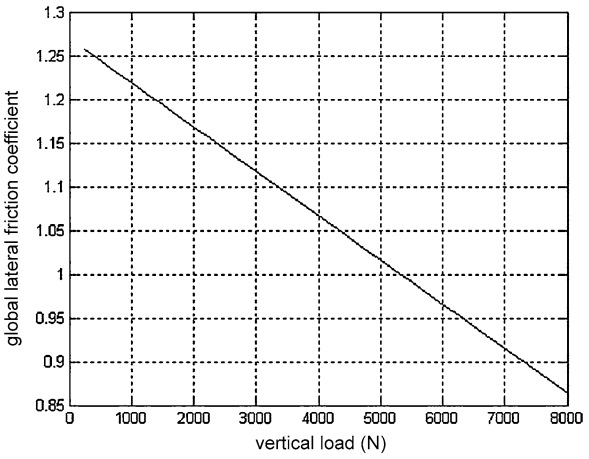

Fig. 2.19 Global lateral friction coefficient μ_p^y vs vertical load F_z

Figure 2.20 shows an example of the vertical moment M_z as a function of the slip angle α, for three values of F_z, that is the plot of $M_z^p(F_z, 0, 0, \alpha, 0)$. The tests are the same of Fig. 2.17 and similar observations apply.

The behavior of $M_z(\alpha)$ is obviously very much affected by the position of the z-axis, which should be always clearly stated. Therefore, it is hard to speak of "typical behavior" of M_z, unless there is general agreement on where to locate the origin O of the reference system. This aspect could be quite relevant in the comparison and interpretation of tests performed by different institutions, particularly for motorcycle tires at large camber angles.

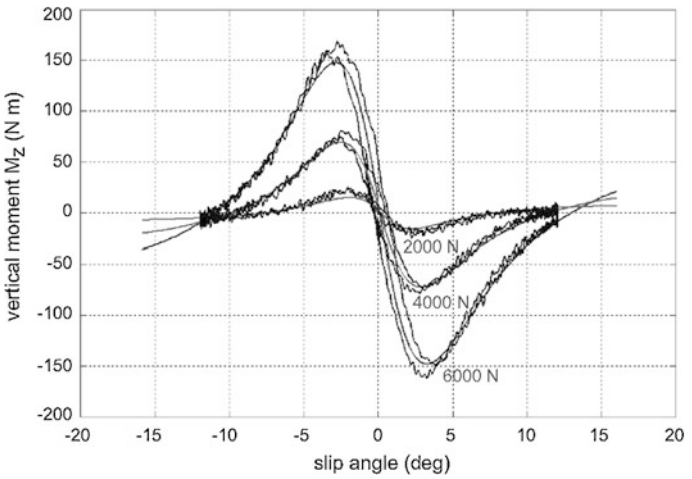

Fig. 2.20 Experimental results: vertical moment M_z vs slip angle α for three values of the vertical load F_z

2.10 Magic Formula

In vehicle dynamics it is useful to have mathematical functions that fit experimental tire response curves, like those in Figs. 2.15 and 2.17. Usually, these curves have similar shapes: they grow less than proportionally, reach a maximum and then tend to a horizontal asymptote. Among the very many functions that share all these features, there is one which is almost exclusively used in vehicle dynamics. It is called *Magic Formula* (MF).

Although, over the years, several versions of the Magic Formula have been developed, they are all based on the following function [14, 16]

$$y(x) = D \sin\{C \arctan[Bx - E(Bx - \arctan(Bx))]\} \tag{2.79}$$

where the four coefficients are usually referred to as

$$\begin{aligned} &B \quad \text{stiffness factor} \\ &C \quad \text{shape factor} \\ &D \quad \text{peak value} \\ &E \quad \text{curvature factor} \end{aligned} \tag{2.80}$$

Of course, y can be either F_x or F_y, with x being the corresponding practical or theoretical slip component.

The Magic Formula belongs to the so-called *empirical tire models*, in the sense that they mimic some experimental curves without any relation to the physical phenomena involved in tire mechanics.

Let $B > 0$. It is quite easy to show that

- $y(0) = 0$ and $y''(0) = 0$, since $y(x) = -y(-x)$ like any anti-symmetric function;
- the slope at the origin is given by $y'(0) = BCD$;
- the value of the horizontal asymptote is $y_a = \lim_{x \to +\infty} y(x) = D \sin(C\pi/2)$, if $E < 1$;
- the function is limited: $|y(x)| \leq D$;
- if $E < 1$ and $1 < C < 2$, then the function has a relative maximum $y_m = y(x_m) = D$, with

$$B(1 - E)x_m + E \arctan(Bx_m) = \tan(\pi/(2C)) \tag{2.81}$$

- $y'''(0) < 0$, if $-(1 + C^2/2) < E$.

Probably, the most relevant features of an experimental curve like in Fig. 2.17 are the peak value y_m with the corresponding abscissa x_m, the asymptotic value y_a and the slope at the origin $y'(0)$. Therefore, to determine the four coefficients a possible procedure is as follows. First set the peak value

$$D = y_m \tag{2.82}$$

then compute the shape factor C employing y_a[13]

$$C = 2 - \frac{2}{\pi} \arcsin\left(\frac{y_a}{D}\right) \tag{2.83}$$

obtain the stiffness factor B as

$$B = \frac{y'(0)}{CD} \tag{2.84}$$

and, finally, determine the curvature factor E from (2.81)

$$E = \frac{\tan(\pi/(2C)) - Bx_m}{\arctan(Bx_m) - Bx_m} \tag{2.85}$$

It is important that $y_a < y_m$. If they are equal (or almost equal), an unexpected plot may result. The Magic Formula usually does a good job at approximating experimental curves, although, with only four coefficients, the fitting may not be of uniform quality at all points. This aspect will be addressed in Figs. 10.16 and 10.17.

Quite often, some coefficients are made dependent on the vertical load F_z. According to Figs. 2.16 and 2.19, the global friction coefficient μ_p decreases almost linearly with F_z, and hence it is quite reasonable to assume

$$D = \mu_p F_z = (a_1 F_z + a_2) F_z \tag{2.86}$$

with $a_1 < 0$. To mimic the pattern shown in Fig. 2.18 for the slope at the origin $y'(0)$, the following formula has been suggested [16]

$$BCD = y'(0) = a_3 \sin\big(2 \arctan(F_z/a_4)\big) \tag{2.87}$$

Typical values may be $a_1 = -0.05\ \mathrm{kN}^{-1}$, $a_2 = 1$, $a_3 = 55$ kN/rad, $a_4 = 4$ kN.

An extensive description of the Magic Formula and all its subtleties can be found in [14].

2.11 Mechanics of Wheels with Tire

The most important aspects of tire behavior can be summarized in a few plots. They are not the whole story, and the interested reader will find in Chap. 10 many hints to better understand steady-state and also transient tire behavior. However, these plots are like a minimum common ground, i.e., something that any vehicle engineer should always have clear in mind.

Of course, they come from tire testing, either indoor or outdoor. Therefore, these plots are like the filtered (smoothed) version of the plots presented in Sect. 2.9. They were drawn employing the Magic Formula with the parameters reported below Eq. (2.87). The shape factor C was set equal to 1.65 for the plots of F_x, and equal to 1.3 for the plots of F_y.

[13] $\sin(C\pi/2) = \sin((2 - C)\pi/2)$, since $1 < C < 2$.

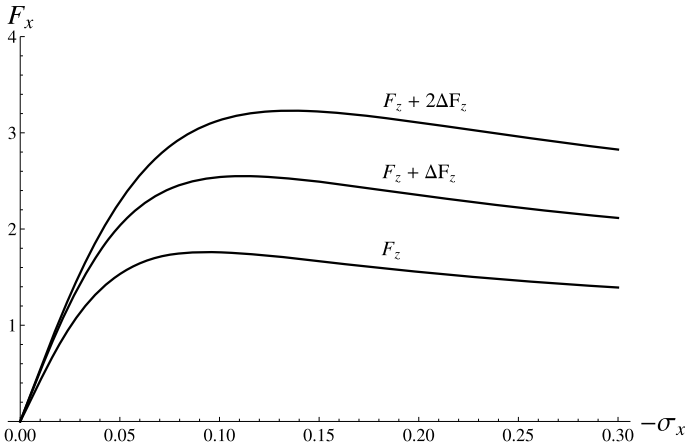

Fig. 2.21 Longitudinal force F_x due to pure longitudinal slip σ_x, for increasing vertical loads F_z. More precisely $F_x = F_x(F_z, 0, \sigma_x, 0, 0)$

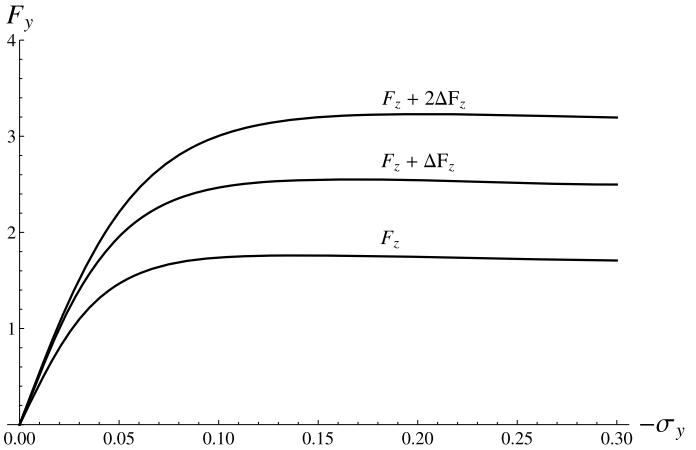

Fig. 2.22 Lateral force F_y due to pure lateral slip σ_y, for increasing vertical loads F_z. More precisely $F_y = F_y(F_z, 0, 0, \sigma_y, 0)$

Most tires under pure longitudinal slip behave like in Fig. 2.21. In particular, the effect of increasing the vertical load F_z is shown. As already mentioned at p. 34, the growth of F_x is less than proportional, particularly for low values of σ_x.

Similarly, most tires under pure lateral slip behave like in Fig. 2.22. In particular, the effect of increasing the vertical load F_z is shown. Again, as already mentioned at p. 35, the growth of F_y is less than proportional, particularly for low values of σ_y. It is precisely this nonlinearity that is, let us say, activated by anti-roll bars to modify the handling set-up of a car.

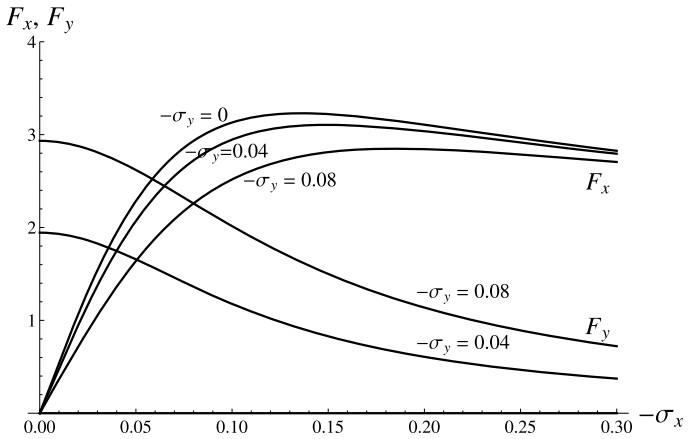

Fig. 2.23 Longitudinal force F_x and lateral force F_y due to combined longitudinal slip σ_x and lateral slip σ_y, for constant vertical load F_z. More precisely $F_y = F_y(F_z, 0, \sigma_x, \sigma_y, 0)$ and $F_y = F_y(F_z, 0, \sigma_x, \sigma_y, 0)$

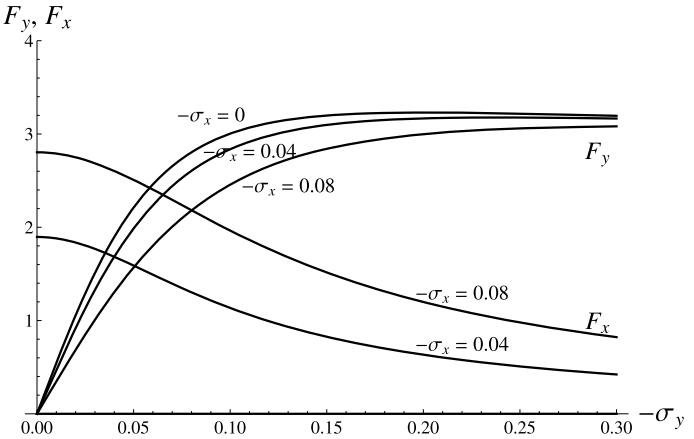

Fig. 2.24 Longitudinal force F_x and lateral force F_y due to combined longitudinal slip σ_x and lateral slip σ_y, for constant vertical load F_z. More precisely $F_y = F_y(F_z, 0, \sigma_x, \sigma_y, 0)$ and $F_y = F_y(F_z, 0, \sigma_x, \sigma_y, 0)$

The simultaneous application of σ_x and σ_y affects the grip forces F_x and F_y the way shown in Figs. 2.23 and 2.24. Basically, the total force $\mathbf{F}_t$, with components F_x and F_y, is directed like the slip vector $\boldsymbol{\sigma}$, with opposite sign, and has a magnitude almost dependent on $|\boldsymbol{\sigma}|$. These aspects will be thoroughly addressed in Chap. 10, were the tire brush model will be developed.

Also very relevant is the effect of the camber angle γ, alone or in combination with σ_y, on the lateral force F_y, as shown in Fig. 2.25 and, for better clarity, also in Fig. 2.26. We see that the camber effects are much stronger at low values of σ_y.

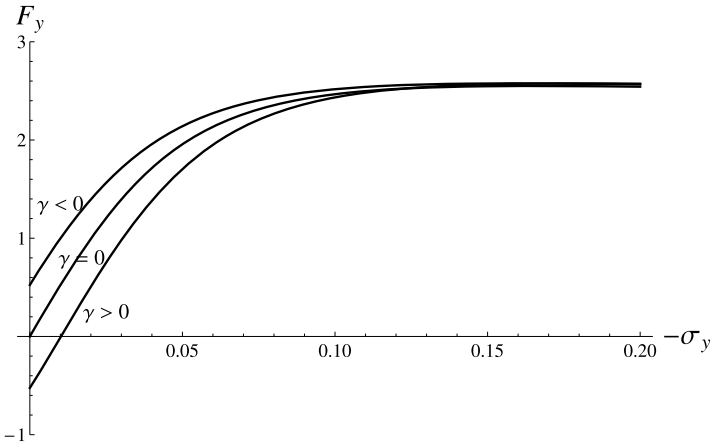

Fig. 2.25 Lateral force F_y due to lateral slip σ_y, for different values of the camber angle γ and constant vertical load F_z. More precisely $F_y = F_y(F_z, \gamma, 0, \sigma_y, 0)$

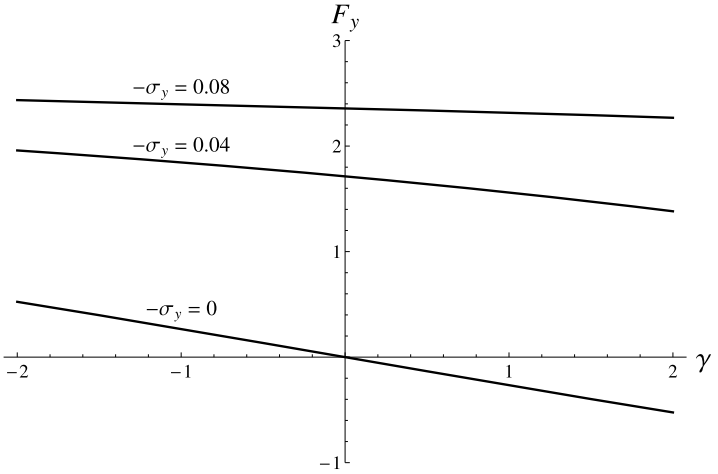

Fig. 2.26 Lateral force F_y due to camber angle γ, for different values of the lateral slip σ_y and constant vertical load F_z. More precisely $F_y = F_y(F_z, \gamma, 0, \sigma_y, 0)$

However, a right amount of camber can increase the maximum lateral force, thus improving the car handling performance.

Finally, the effect of the increasing the grip coefficient μ is investigated. We see in Figs. 2.27 and 2.28 that, as expected, we get higher maximum tangential forces. However, it should also be noted that changing the grip does not affect the slope of the curves near the origin.

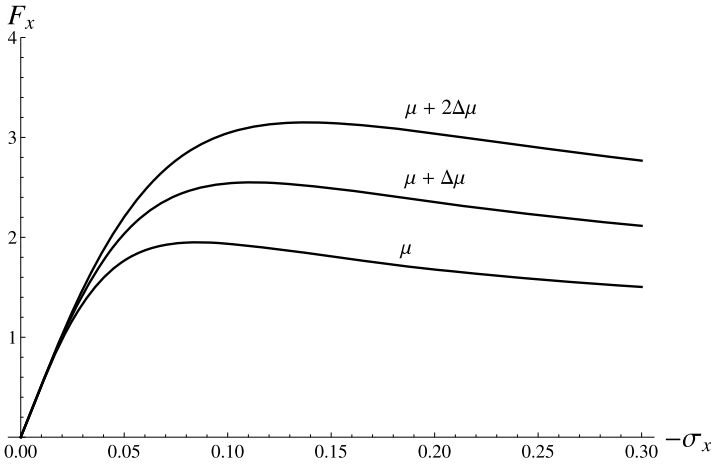

Fig. 2.27 Longitudinal force F_x due to pure longitudinal slip σ_x, for constant vertical load F_z and increasing grip

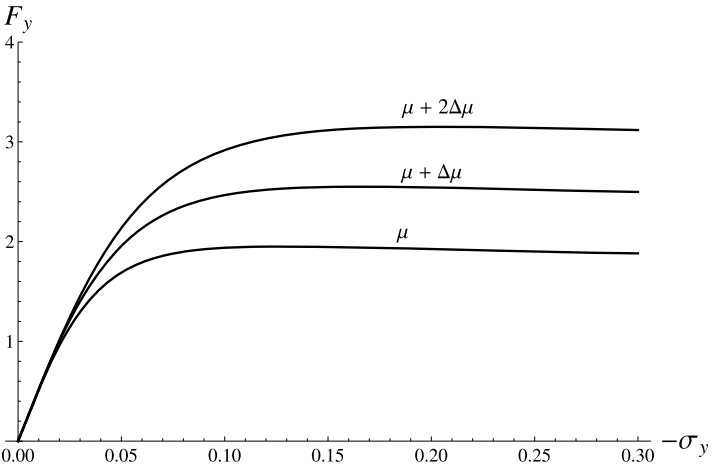

Fig. 2.28 Lateral force F_y due to pure lateral slip σ_y, for constant vertical load F_z and increasing grip

2.12 Summary

In this chapter we have first pursued the goal of clearly describing the relevant kinematics of a wheel with tire, mainly under steady-state conditions. This had led to the definitions of slips as a measure of the extent to which the wheel with tire departs from pure rolling conditions. The slip angle has been also defined and discussed. It has been shown that a wheel with tire resembles indeed a rigid wheel because slip angles are quite small. Tire experimental tests shows the relationships between the

kinematics and the forces/couples the tire exchanges with the road. The Magic Formula provides a convenient way to represent these functions. Finally, the mechanics of the wheel with tire has been summarized with the aid of a number of plots.

2.13 List of Some Relevant Concepts

p. 8 a wheel with tire is barely a wheel;
p. 11 there are two distinct contributions to the spin velocity of the rim;
p. 11 in a wheel, longitudinal velocities are expected to be much higher than lateral ones;
p. 15 the name "self-aligning torque" is meaningless and even misleading;
p. 21 rim kinematics depends on six variables, but often (not always) only five may be relevant for the tire;
p. 22 a reasonable definition of pure rolling for a wheel with tire is that the grip actions $\mathbf{t}$ have no global effect;
p. 20 pure rolling and free rolling are different concepts;
p. 27 tire slips measure the distance from pure rolling;
p. 30 tire slips do not provide any direct information on the amount of sliding at any point of the contact patch;
p. 32 tire forces and moments depend on both the camber angle γ and the spin slip φ.

References

1. Bastow D, Howard G, Whitehead JP (2004) Car suspension and handling, 4th edn. SAE International, Warrendale
2. Bergman W (1977) Critical review of the state-of-the-art in the tire and force measurements. SAE Preprint (770331)
3. Clark SK (ed) (2008) The pneumatic tire. NHTSA–DOT HS 810 561
4. Dixon JC (1991) Tyres, suspension and handling. Cambridge University Press, Cambridge
5. Font Mezquita J, Dols Ruiz JF (2006) La Dinámica del Automóvil. Editorial de la UPV, Valencia
6. Gillespie TD (1992) Fundamentals of vehicle dynamics. SAE International, Warrendale
7. Meirovitch L (1970) Methods of analytical dynamics. McGraw-Hill, New York
8. Michelin (2001) The tyre encyclopaedia. Part 1: grip. Société de Technologie Michelin, Clermont–Ferrand [CD-ROM]
9. Michelin (2002) The tyre encyclopaedia. Part 2: comfort. Société de Technologie Michelin, Clermont–Ferrand [CD-ROM]
10. Michelin (2003) The tyre encyclopaedia. Part 3: rolling resistance. Société de Technologie Michelin, Clermont–Ferrand [CD-ROM]
11. Milliken WF, Milliken DL (1995) Race car vehicle dynamics. SAE International, Warrendale
12. Murray RM, Li Z, Sastry SS (1994) A mathematical introduction to robot manipulation. CRC Press, Boca Raton
13. Pacejka HB (1996) The tyre as a vehicle component. In: 26th FISITA congress '96: engineering challenge human friendly vehicles, Prague, June 17–21, pp 1–19

14. Pacejka HB (2002) Tyre and vehicle dynamics. Butterworth–Heinemann, Oxford
15. Pacejka HB (2005) Slip: camber and turning. Veh Syst Dyn 43(Supplement):3–17
16. Pacejka HB, Sharp RS (1991) Shear force development by pneumatic tyres in steady state conditions: a review of modelling aspects. Veh Syst Dyn 20:121–176
17. Popov VL (2010) Contact mechanics and friction. Springer, Berlin
18. Pytel A, Kiusalaas J (1999) Engineering mechanics—statics. Brooks/Cole, Pacific Grove
19. Wong JY (2001) Theory of ground vehicles. Wiley, New York

http://www.springer.com/978-94-017-8532-7

The Science of Vehicle Dynamics
Handling, Braking, and Ride of Road and Race Cars
Guiggiani, M.
2014, XII, 356 p. 255 illus., Hardcover
ISBN: 978-94-017-8532-7